Pergamon

Int. J. Heat Mass Transfer. Vol. 38, No. 7, pp. 1249–1259, 1995

0017-9310/95 $9.50+0.00

0017-9310(94)00254-1

Three-dimensional convection in rectangular domains with horizontal throughflow

E. SCHRÖDER and K. BÜHLER

Institut für Strömungslehre und Strömungsmaschinen, Universität Karlsruhe, D-76128 Karlsruhe, Germany

(*Received* 22 *March* 1994 *and in final form* 20 *July* 1994)

Abstract—The Rayleigh–Bénard convection with a superimposed horizontal shear flow in rectangular domains is treated numerically utilizing a finite difference method and experimentally by applying an interferometric measuring technique. The fluid used is silicon oil, a high Prandtl number fluid, $Pr = 530$. The investigations concern the supercritical Rayleigh number region of $2300 \leqslant Ra \leqslant 20\,000$. The Reynolds number, which characterizes the strength of the throughflow, varies in the range of $3 \times 10^{-5} \leqslant Re \leqslant 0.1$. According to special parameter combinations of the Rayleigh and the Reynolds number, convective rolls with different orientations can be distinguished. The dynamical behavior of travelling, transverse rolls is also considered.

INTRODUCTION

The Rayleigh-Bénard problem with a superimposed mass flux in the laminar flow region is of principal as well as of practical interest. New questions arise from the chemical vapor deposition (CVD) in the microelectronic industry, where the Reynolds number is in the order of $Re \leqslant 200$ [1]. The knowledge of the flow structure in CVD reactors is necessary to avoid inhomogeneities in the deposition of silicon.

The following section describes convective flow in rectangular domains with rigid boundaries. In the absence of a shear flow a Newtonian, incompressible fluid is heated from below and cooled from above. As a consequence of this temperature distribution, a macroscopic movement of the fluid sets in, when the Rayleigh number exceeds a critical value. The critical Rayleigh number depends on the geometry of the domain and the thermal and hydrodynamic boundary conditions. For example, in a short box with the aspect ratios of $h_x/h_z = 7.4$, $h_y/h_z = 4.1$ and perfectly conducting sidewalls, the critical Rayleigh number is about $Ra_{crit} = 1950$ for the onset of convection [2]. The flow patterns in the supercritical Rayleigh number region are rolls, which are orientated in a transverse direction, i.e. parallel to the shorter side of a rectangular box as shown by Stork and Müller [3]. The reason is that the critical Rayleigh number of longitudinal rolls, i.e. rolls parallel to the longer side of a rectangular box or a channel, is higher than the critical Rayleigh number of transverse rolls. For example, in a channel with an aspect ratio of $h_y/h_z = 4.0$ and isolated sidewalls, the critical value is $Ra_\perp = 1718.45$ for the onset of convection in the shape of transverse rolls, for longitudinal rolls the critical Rayleigh number $Ra_\parallel$ amounts to $Ra_\parallel = 1810.48$ [4]. Without throughflow, the supercritical state is called free convective state.

The stability of convection with a superimposed throughflow in long channels is considered by Platten and Legros [4]. Here, the rolls can either align in transverse direction if the Reynolds number is low, shown in Fig. 1(a), or they can be oriented in longitudinal direction, Fig. 1(b), i.e. in the direction of the shear flow, when the Reynolds number exceeds a certain critical value Re^*, which depends on the aspect ratio and increases with decreasing Prandtl number. The experimental investigations of Luijkx *et al.* [5]

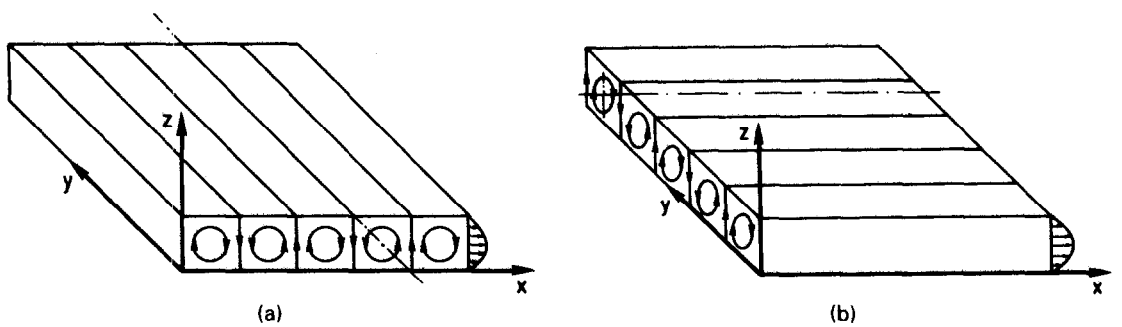

Fig. 1. (a) Transverse rolls; (b) longitudinal rolls.

NOMENCLATURE

f	oscillation frequency, non-dimensionalized by κ/h_z^2
g	gravity constant
h_x, h_y, h_z	length, depth, height of the box/channel section
l	length of the inlet and outlet chamber
p^*	non-dimensional pressure
P_x	non-dimensional pressure gradient
Pr	Prandtl number, ν/κ
Ra	Rayleigh number, $\alpha g \Delta T h_z^3/(\nu\kappa)$
$Ra_\perp$	critical Rayleigh number for the development of transverse rolls
$Ra_\parallel$	critical Rayleigh number for the development of longitudinal rolls
Re	Reynolds number, $\bar{u}h_z/\nu$
t	time
T	non-dimensional temperature
T_u	temperature of the bottom plate
T_o	temperature of the top plate
$\bar{u}$	average velocity of the shear flow
u_r	travelling velocity of the transverse rolls
u, v, w	velocity components
$\mathbf{v}$	velocity vector
$\dot{V}$	volume flux
x, y, z	coordinates.

Greek symbols

α	thermal expansion coefficient
β	aspect ratio, h_y/h_z
ε	porosity
κ	temperature conductivity
λ	average wavelength
λ_c	critical wavelength according to two horizontal, rigid boundaries
ν	kinematic viscosity
τ	time, non-dimensionalized by h_z^2/κ.

were performed utilizing silicon oil ($Pr = 450$) and a channel with an aspect ratio of $\beta = 5.25$ and a critical Reynolds number of $Re^* = 6.4 \times 10^{-3}$. Their results show, that the critical Rayleigh number $Ra_\perp$ of transverse rolls increases with increasing Reynolds number. The critical Rayleigh number $Ra_\parallel$ of longitudinal rolls is unaffected by the throughflow, but is still a function of the aspect ratio of the channel. Therefore, a Reynolds number exists, below which transverse rolls exist and above which longitudinal rolls can be found. In the transverse case, the rolls travel downstream with a certain velocity u_r, which is slightly greater than the average velocity $\bar{u}$ of the shear flow.

Ouazzani *et al.* [6, 7] proved, that $u_r/\bar{u}$ is independent of the Reynolds number but a function of the Rayleigh number. They also considered the amplitude of the vertical velocity in the case of transverse rolls as well as in the case of longitudinal rolls. For both, they found the convective amplitude, represented by the vertical velocity w, to be independent of the Reynolds number. Müller [8] considered the two-dimensional flow in different geometries. In short channels he could distinguish between absolute and convective instability. Phase fixing boundary conditions cause a stationary state of transverse rolls even in the case of a superimposed shear flow. A noise source at the inlet boundary causes the appearance of transverse rolls even in the convective unstable flow region.

EXPERIMENTAL INVESTIGATIONS

The convection with a superimposed mass flux is experimentally investigated in a short box, shown in Fig. 2, having aspect ratios of $h_x/h_z = 7.4$ and $h_y/h_z = 4.1$. Between two copper plates placed at the bottom and the top of the box and which are kept at constant, but different temperatures, a glass frame is situated forming the lateral sidewalls. Inside the frame, two porous plexiglass plates (porosity $\varepsilon = 0.37$) separate the measuring part from a small inlet and outlet chamber ($l/h_y = 1.36$). The fluid, silicon oil M50, $Pr = 530$, enters the inlet chamber via a hole in the bottom plate, passes the porous sidewall, flows through the measuring part, passes the porous sidewall at the outlet, reaches the outlet chamber (same geometry as the inlet chamber), and leaves the box through a hole in the upper plate. A geared pump assures, that the fluid flow has no pulsation. The strength of the throughflow is measured by a flowmeter outside the box. The room is held at constant temperature T_m, the average temperature between the top and the bottom plate.

The measuring techniques used are the whole-field differential interferometry [9] and the laser differential interferometry. The first method is used to visualize the density field in the whole box, the latter method allows to measure the velocity and the frequency of the travelling, transverse rolls in the middle of the box. In addition, a light sheet method enables to visualize the flow structure in different planes to get a three-dimensional impression of the flow.

The temperature difference between the top and bottom plate has an accuracy of 0.06 K during a time of 30 h, the minimal temperature difference was $\Delta T_{min} = 0.7$ K. The relative error of the Rayleigh and the Reynolds number is about 10% during the whole measuring time. At first a stationary free convective state with six to eight transverse rolls is established by

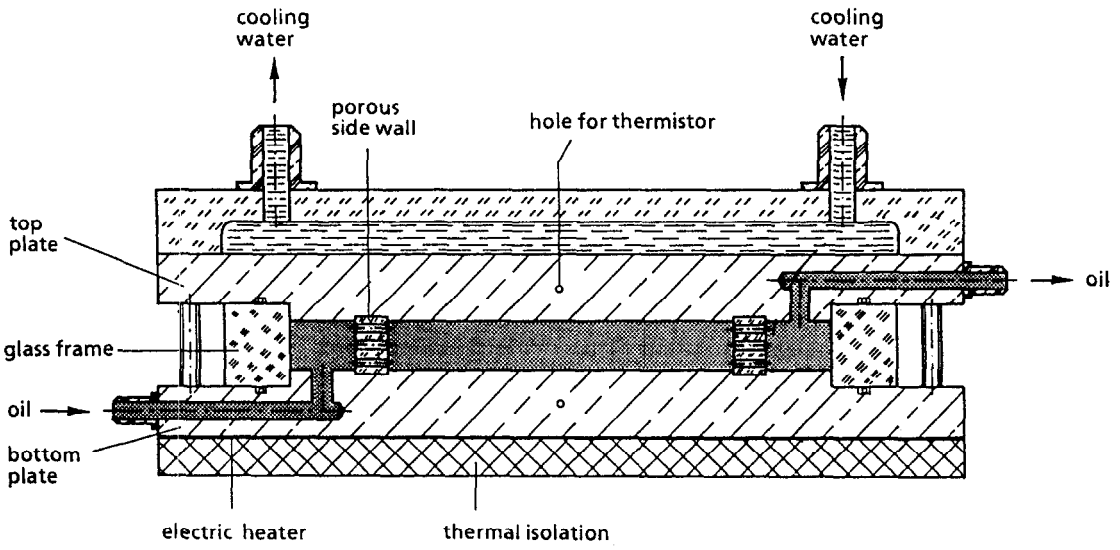

Fig. 2. Measuring cell.

heating up and cooling the box for about 5 h, then the shear flow is superimposed and the dynamical behavior of the mixed convection analyzed.

At Rayleigh numbers $Ra > Ra_{\parallel}$ hysteresis effects may occur if another initial condition, i.e. start with the shear flow before heating up and cooling the box, is chosen, but this effect is not discussed in the present paper. Some investigations on hysteresis effects are described in ref. [7].

NUMERICAL INVESTIGATIONS

The numerical investigations concern the superposition of a supercritical convective state with a lateral throughflow in two different geometries, i.e. a short box with the aspect ratios of $h_x/h_z = 7.4$; $h_y/h_z = 4.1$ and a long box with the aspect ratios of $h_x/h_z = 29.6$; $h_y/h_z = 4.1$. A scheme of the geometry is shown in Fig. 3. The non-dimensional mass, impulse, and energy conservation equations are simplified by the Boussinesq approximation. The used time scale is the thermal diffusion time h_z^2/κ, the length scale is h_z and T represents $(T-T_m)/(T_u-T_o)$ where T_u and T_o are the temperatures of the bottom and the top plate and $T_m = (T_u+T_o)/2$. The Boussinesq equations are written in the following, non-dimensional form

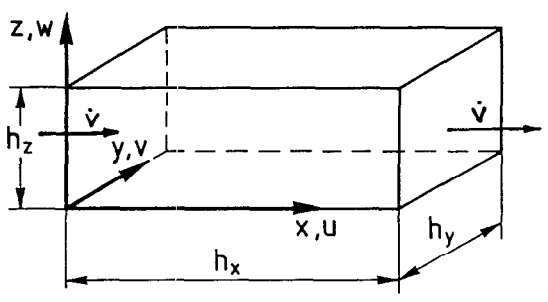

Fig. 3. Scheme of the geometry.

$$\nabla \cdot \mathbf{v} = 0 \tag{1}$$

$$\frac{\partial \mathbf{v}}{\partial t} + (\mathbf{v}\cdot\nabla)\cdot\mathbf{v} = -\nabla p^* + Pr\cdot\Delta\mathbf{v} + Ra\cdot Pr\cdot T\cdot\mathbf{e}_z \tag{2}$$

$$\frac{\partial T}{\partial t} + (\mathbf{v}\cdot\nabla)\cdot T = \Delta T. \tag{3}$$

The boundaries are considered to be perfectly heat conducting, i.e. the top and bottom boundaries are set at constant temperatures, the temperature distribution of all other boundaries, including the inlet and outlet, is assumed to be linear. The non-slip condition is applied to describe the hydrodynamic boundary conditions for all boundaries. To simulate the lateral shear flow through porous sidewalls, a constant velocity profile is assumed at the inlet and outlet.

Table 1 gives an overview of the non-dimensional boundary conditions. The initial conditions are stationary free convective states at supercritical Rayleigh numbers. The stationary free convective states can be achieved either from a purely heat conducting state or from a state at rest at constant average temperature $T_m = 0$.

The used numerical method is an explicit finite difference method according to the MAC-method described by Amsden and Harlow [10]. It has been developed for three-dimensional, free convection by Kirchartz [11]. The differencing scheme is implemented on a staggered grid using a DuFort–Frankel differencing scheme for the treatment of the viscous terms. Second order accuracy for time and space discretization can be afforded.

The grid size is set to $\Delta x : \Delta y : \Delta z = 0.0925 : 0.105 : 0.0625$, the maximum time step is $\Delta\tau \leqslant 10^{-3}$ to guarantee second-order accuracy of the finite differencing scheme.

RESULTS

The flow structure of free convection with superimposed mass flux in rectangular domains can be sub-

Table 1. Boundary conditions for convection in rectangular domains with lateral throughflow

Boundaries	Coordinates	Thermal boundary condition	Hydrodynamic boundary condition
Top	$z = 1$	$T = -0.5$	$u = v = w = 0$
Bottom	$z = 0$	$T = 0.5$	$u = v = w = 0$
Front, rear side	$y = 0; 1$	$T = 0.5 - z$	$u = v = w = 0$
Inlet, outlet	$x = 0; 1$	$T = 0.5 - z$	$v = w = 0, u = Re \cdot Pr$

divided into three parts characterized by the Reynolds number at a fixed Rayleigh number. At first the structure and the dynamical behavior of the flow patterns in the short box is discussed. Then the results are compared to the convective states in the long box.

Short box

(a) $\mathrm{Re} < 10^{-4}$. The inlet and outlet boundaries force a phase fixing of the flow structure. Depending on the initial wavelength, one or two rolls disappear at the outlet, then the structure remains stationary. No movement of the transverse rolls can be established after one day. The structure remains unchanged during 24–30 h.

At the free convective state, the box is filled with six to eight transverse rolls, i.e. a wavelength between $\bar{\lambda} = 1.85$ and $\bar{\lambda} = 2.467$ as a consequence of the initial condition. Here, $\bar{\lambda}$ is the non-dimensional, average wavelength.

At the entrance, the rolls change their orientation and get a longitudinal character. With increasing Rayleigh number, a higher Reynolds number is necessary to cause a roll displacement. Figure 4 separates the stationary and the oscillating states. In the oscillating region the rolls move downstream with a certain velocity u_r. The travelling rolls cause an oscillating change of the vertical velocity w at a fixed point of the box with a certain frequency f discussed in the following section.

(b) $10^{-4} \leqslant \mathrm{Re} < 3 \times 10^{-3}$. In this parameter range, the rolls travel downstream with a certain velocity u_r depending on the average velocity $\bar{u}$ of the throughflow. The investigations start from a stationary free convective state with seven rolls and an upstream zone at the entrance. Figure 5 shows the electrical signal obtained by the laser differential interferometer. The laser beam is localized in the middle of the box, i.e. at $h_x/2$ and $h_z/2$. The density differences are too high to measure on one flank of the $\cos^2$-curve of the light intensity signal. Therefore, the signal has no cosine profile. The symbols indicate the roll centers passing by the interferometer. Below the experimental signal the numerical simulation of the laser differential signal in the middle of the box is given, Fig. 6. The comparison shows that the amplitudes of the electrical signal, represented in the number of changes of the signal from the maximum to the minimum value between the roll centers, are nearly equal.

The frequency of the oscillations is compared in addition. The dimensionless frequency of the experimental signal is about $f = 0.244$, the numerical simulation predicts a frequency of $f = 0.235$. Figure 7 shows that the frequency is a linear function of the Reynolds number. The symbols indicate the experimental results, the line represents a fit of the numeri-

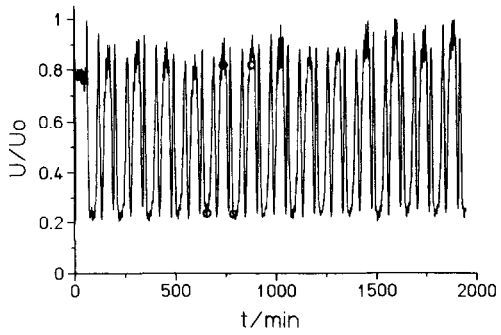

Fig. 5. Electrical signal (voltage) of the laser differential interferometer, $Ra = 3300$, $Re = 7 \times 10^{-4}$, $Pr = 530$.

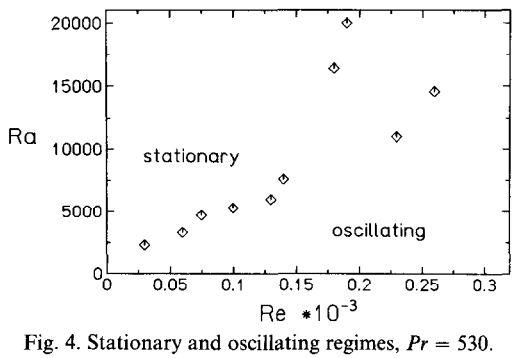

Fig. 4. Stationary and oscillating regimes, $Pr = 530$.

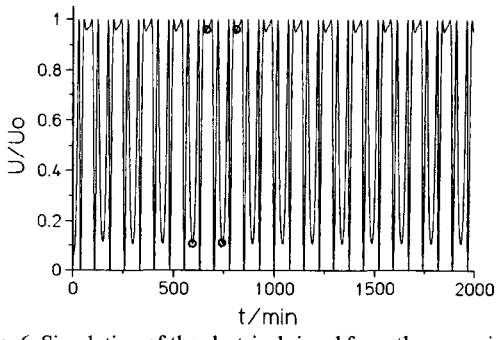

Fig. 6. Simulation of the electrical signal from the numerical temperature data.

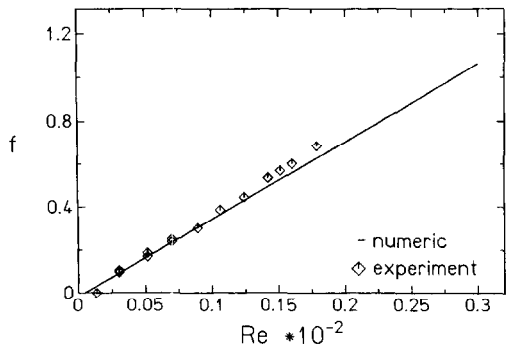

Fig. 7. Frequency of the travelling, transverse rolls as function of Re, $Ra = 3300$, $Pr = 530$.

cal calculations. As shown in Fig. 7, the straight line does not pass the origin of the coordinate system, proving that phase fixing of the roll structure is existent.

The numerical oscillation frequency for different Rayleigh and Reynolds numbers is shown in Fig. 8. The derivative of the straight lines is becoming smaller at higher Rayleigh numbers. None of the straight lines passes the origin of the coordinate system, so that phase fixing is present in all cases. At high Rayleigh numbers ($Ra > 14\ 000$) the frequency varies only slightly with increasing Rayleigh numbers. The reason is, that at high Rayleigh numbers the convective amplitude rises only slightly with increasing Rayleigh numbers, so that the influence of the convective motion on the travelling velocity becomes less important.

The wavelength of the travelling, transverse rolls is not uniform over the length of the box. Near the entrance region the rolls are deformed in the way that they get a longitudinal character. At the outlet, the roll diameter tends to become smaller, especially when the last roll is squeezed through the porous sidewall.

Figures 9(a)–(d) show the flow structure over one period of time. At the inlet, the rolls turn out to be longitudinal, at the outlet transversal. Near the middle of the box, the different forms are connected by a mixed flow region. During one period of time the transverse rolls travel downstream and disappear at the outlet. After the disappearence of two rolls at the outlet, a new pair of transverse rolls is formed in the mixed flow region. They expand while travelling downstream. The non-uniformity of the wavelength makes it impossible to calculate a uniform travelling velocity on the basis of the frequency data.

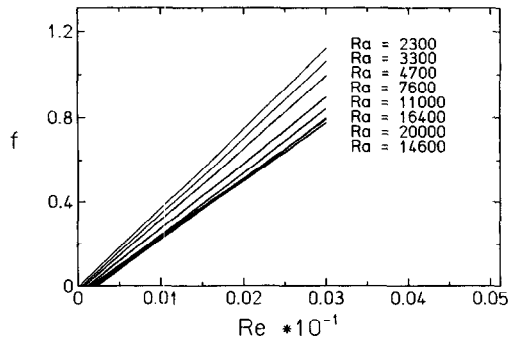

Fig. 8. Frequency as function of Ra and Re, numerical results.

(c) $3 \times 10^{-3} \leqslant Re \leqslant 0.1$. When the Reynolds number is raised, the longitudinal part near the entrance enlarges. At least it fills the whole box. Transverse structures are no longer visible. The flow still remains instationary, shown in Fig. 10, but the amplitude becomes smaller by increasing the Reynolds number. The reason is, that either transverse structures, caused by the lateral sidewalls, still exist, or that disturbances at the entrance region are reinforced and pushed downstream. The frequency still rises with increasing Reynolds number.

Long box

(a) *Analysis of the frequency.* To prove whether the length of the box has any influence on the dynamical behavior of the mixed convection or not, the box is enlarged. Figure 11 shows the frequency as a function of the Reynolds number. Compared to the short box, the phase fixing of the roll structure takes place in the long box at lower Reynolds numbers. In addition the results of the investigations in infinitely long geometries (channel) are given and discussed in the next section. The symbols indicate the numerical results, the straight lines are fits of those calculations. In the long box, the rolls are displaced easier than in the short box which leads to higher frequencies. At high Reynolds numbers, the frequencies of the short and of the long box become more similar. The straight lines intersect with each other in the parameter range, where the roll structure in the short box is completely longitudinal.

(b) *Analysis of the roll structure.* The starting point here is a free convective state with 33 rolls and an average wavelength of $\bar{\lambda} = 1.79$, shown in Fig. 12. For the mixed convective state the wavelength changes to $\bar{\lambda} = 2.42$, at Reynolds numbers $Re < 1.42 \times 10^{-3}$, shown in Fig. 13. At higher Reynolds numbers, the rolls get more compressed, resulting in a wavelength of $\bar{\lambda} = 2.3$. The experiments of Luijkx *et al.* [5] show a wavelength of $\bar{\lambda} = 2.2$ in the case of travelling, transverse rolls, which is in good agreement with the here reported results.

In the Reynolds number range of $3 \times 10^{-3} \leqslant Re \leqslant 5 \times 10^{-3}$ the roll structure in the long box turns out to be longitudinal as shown in Fig. 14. The change of the orientation follows in the same way as in the short box, i.e. the development of mixed forms of transverse and longitudinal rolls is possible.

SPECIAL CASE

This section gives some additional results of convection with superimposed throughflow in an infinitely long channel at an aspect ratio of $h_y/h_z = 4.1$.

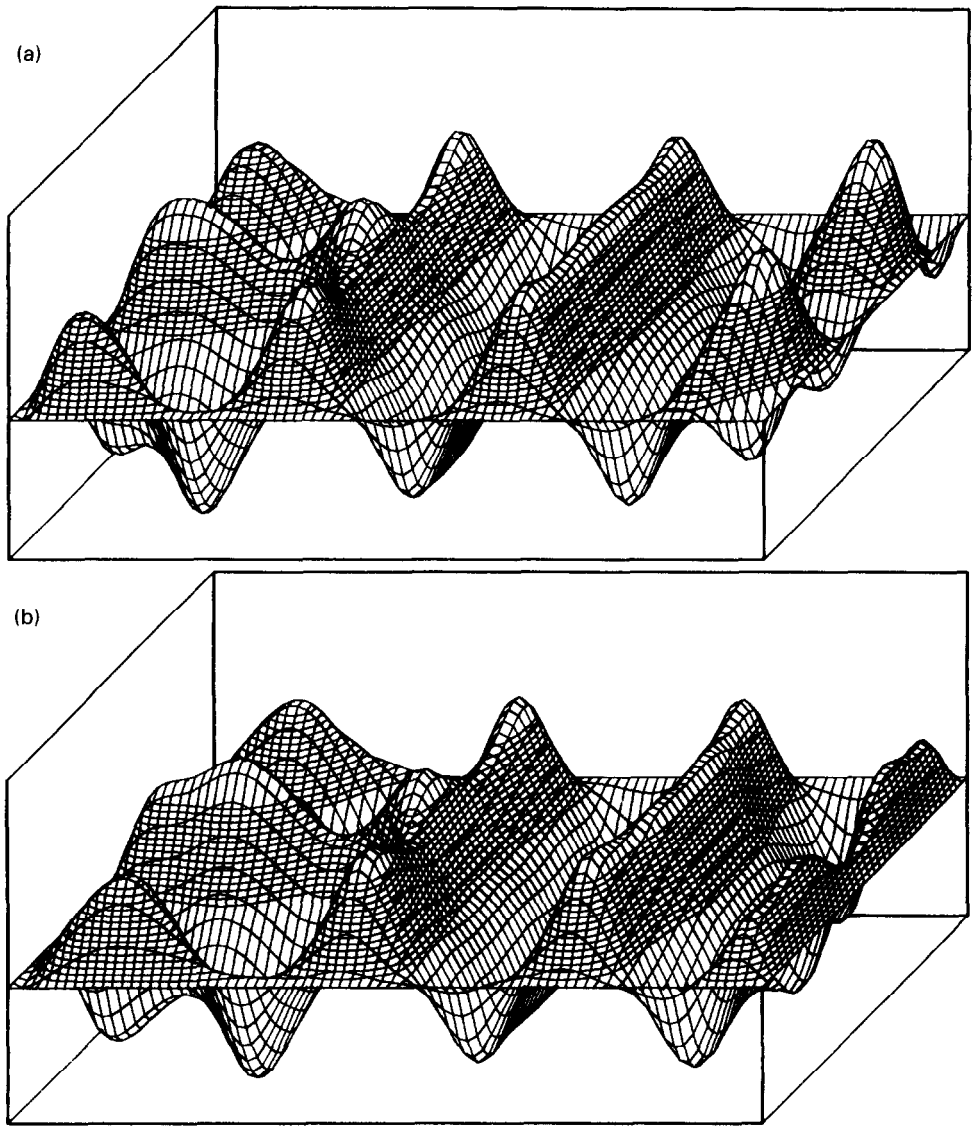

Fig. 9. (a) Vertical velocity at $\tau = 34.72$, $Ra = 7600$, $Re = 1.06 \times 10^{-3}$, $Pr = 530$, left side: inlet, right side: outlet; (b) vertical velocity at $\tau = 35.74$; (c) vertical velocity at $\tau = 36.77$; (d) vertical velocity at $\tau = 37.79$.

The length of the investigated channel section is $h_x/h_z = 8.063$.

To avoid inflow and outflow effects, periodic boundary conditions are used as inlet and outlet conditions for the numerical investigations. To simulate the throughflow, equation (2) must be completed by an additional pressure gradient.

$$\frac{\partial \mathbf{v}}{\partial t} + (\mathbf{v} \cdot \nabla) \cdot \mathbf{v} = -\nabla p^* + Pr \cdot \Delta \mathbf{v} - P_x \cdot \mathbf{e}_x + Ra \cdot Pr \cdot T \cdot \mathbf{e}_z$$

$$P_x = -2 \cdot Re \cdot Pr^2 \cdot H_y \cdot \left[\frac{H_y}{6} - 32 \sum_{n=1,3,5,\ldots}^{\infty} \frac{\tanh\left(n\pi \frac{H_y}{2}\right)}{(n\pi)^5} \right]^{-1} . \quad (4)$$

P_x can be derived from the analytical solution of a three-dimensional channel flow [4]. All other boundary conditions are the same as those given in Table 1.

The initial condition here is, according to the investigations discussed earlier, a stationary free convective state with eight rolls. Periodic boundary conditions allow only an even number of rolls. The wavelength of the free convective state is set to the critical wavelength of a system with two horizontal, rigid boundaries, i.e. $\lambda_c = 2.02$. Therefore, the periodic length is given to $4 \cdot \lambda_c$. According to the Reynolds number, different flow patterns can be analyzed.

(a) *Small Reynolds numbers*, $\mathrm{Re} \to 0$. Phase fixing is not possible in this system. No stationary mixed convective state can be found in a system where periodic boundary conditions are assumed.

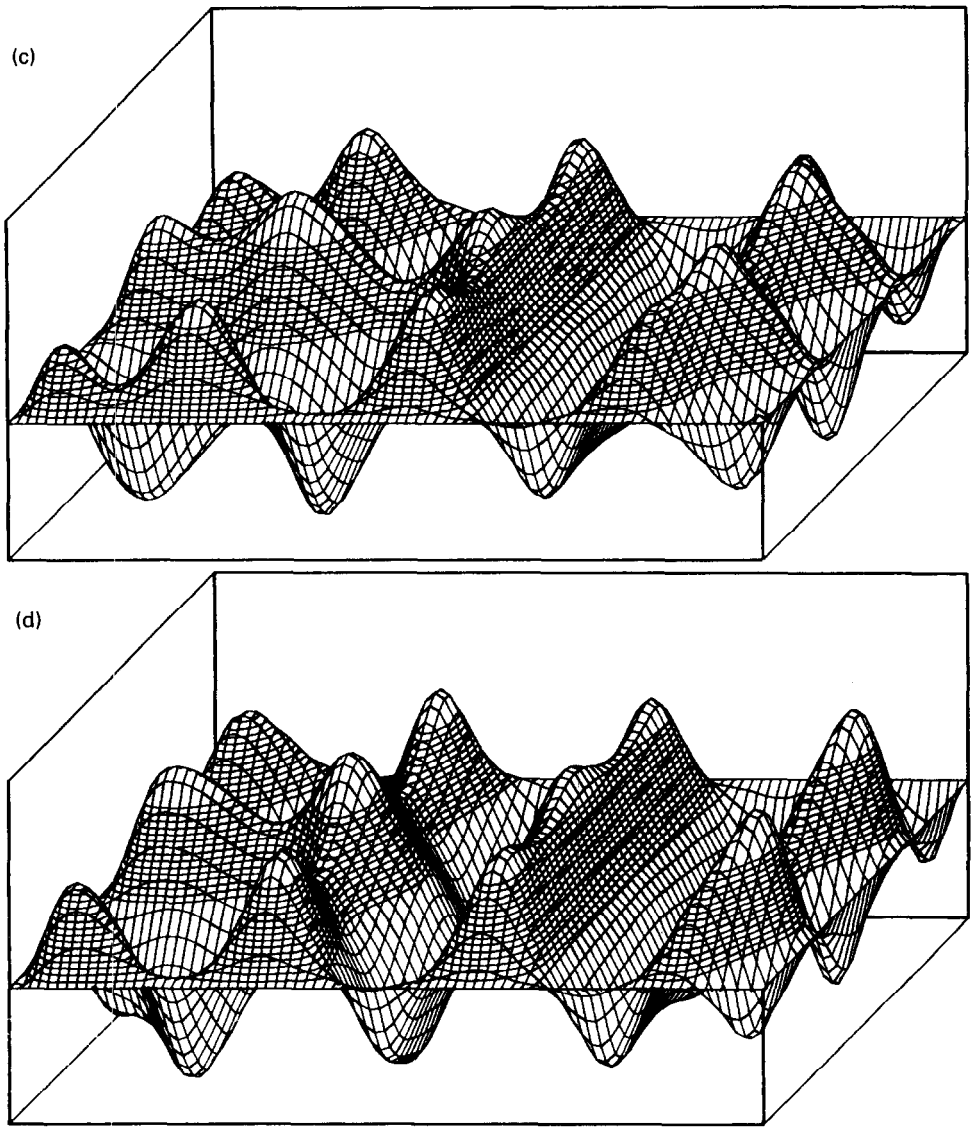

Fig. 9—*continued.*

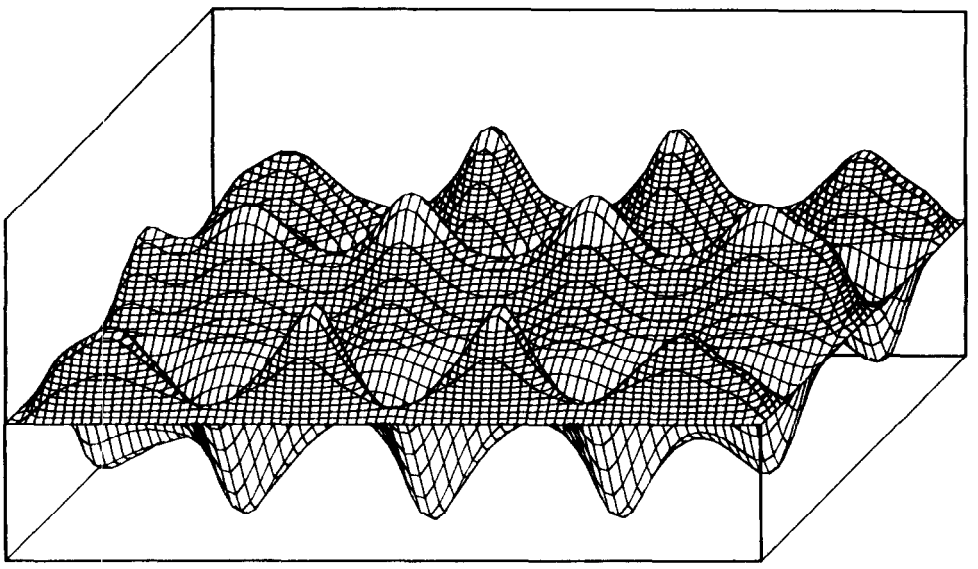

Fig. 10. Vertical velocity of the longitudinal rolls, $Ra = 14\,600$, $Re = 2.7 \times 10^{-3}$, $Pr = 530$.

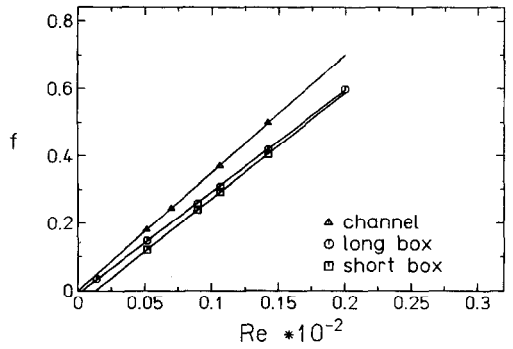

Fig. 11. Frequencies as function of *Re* for three different systems.

The uniqueness of the wavelength allows to calculate the travelling velocity in the following way: $u_r = f \cdot \lambda$. The quotient $u_r/\bar{u}$ does not depend on the Reynolds number, but is a linear function of the Rayleigh number, if $Ra < 5000$. Some approximations of $u_r/\bar{u}$ are given in Table 2, where the equations of the here applied approximations and the approximations given in refs. [6, 7] are compared. One can find out that $u_r/\bar{u}$ is always greater than one.

The analysis of the convective amplitude w_{max} shows that w_{max} is independent of the Reynolds number. Increasing the Rayleigh number, $w_{max} \sim \sqrt{Ra}$ can be obtained. This is true for small Reynolds numbers, i.e. $Ra < 5000$.

The flow structure of the travelling, transverse rolls

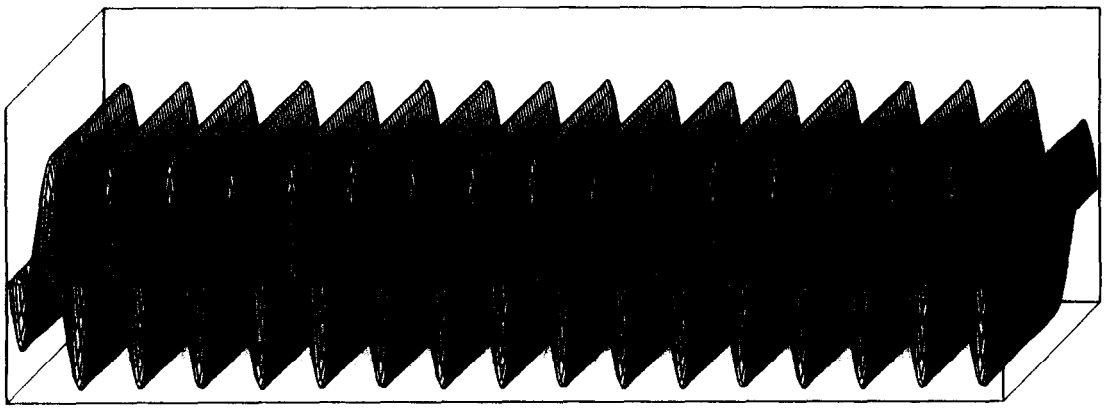

Fig. 12. Vertical velocity of the mixed convection in a long box, $Ra = 7600$, $Re = 0$, $Pr = 530$.

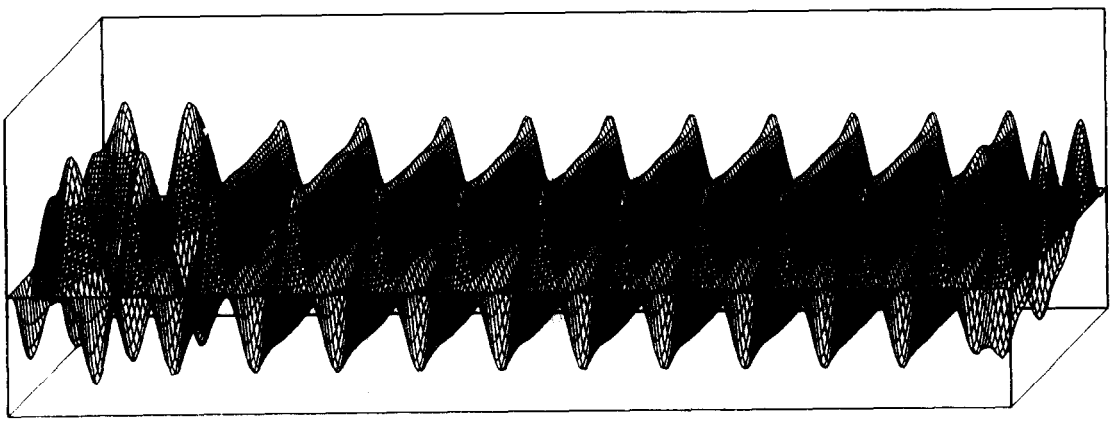

Fig. 13. Vertical velocity of the mixed convection in a long box, $Ra = 7600$, $Re = 0.89 \times 10^{-3}$, $Pr = 530$.

(b) $\mathrm{Re} \leqslant 0.05$. The frequency of the travelling transverse rolls is still a linear function of the Reynolds number, shown in Fig. 15. The increasing Rayleigh number enlarges the convective amplitude and reduces the oscillation frequency. The wavelength does not vary along the channel length, therefore its value is the critical one everywhere in the channel. The Reynolds number dependence of the frequency can be eliminated and the reduced frequency is only a function of the Rayleigh number, shown in Fig. 16.

in a long channel is different from the structure discussed above. Here no mixed flow regions are possible, i.e. a mixture of longitudinal and transverse rolls. The rolls remain pure transverse in a certain range of parameters.

(c) $\mathrm{Re} > 0.05$. In this parameter range the flow structure changes. The transverse rolls are deformed simultaneously in the whole channel in the way that the axes get curved as illustrated in Fig. 17. Increasing the Reynolds number to $Re > 0.1$ leads to purely

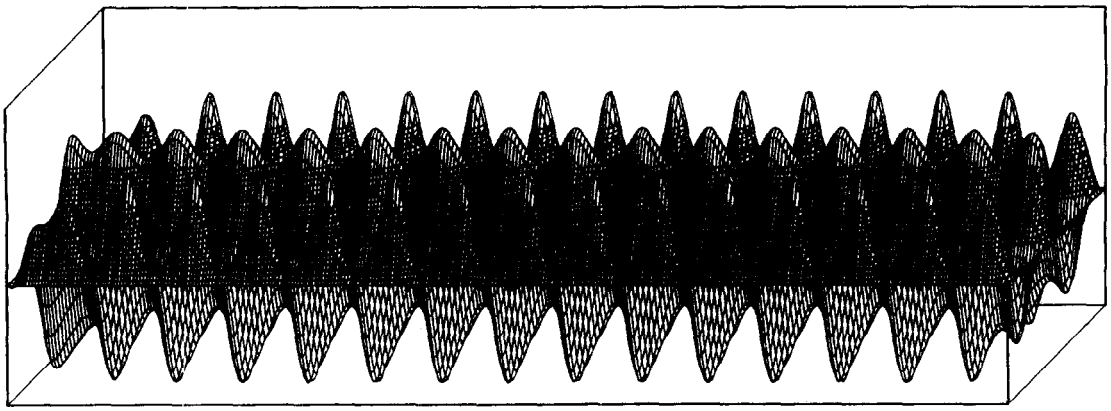

Fig. 14. Vertical velocity of the mixed convection in a long box, $Ra = 7600$, $Re = 5 \times 10^{-3}$, $Pr = 530$.

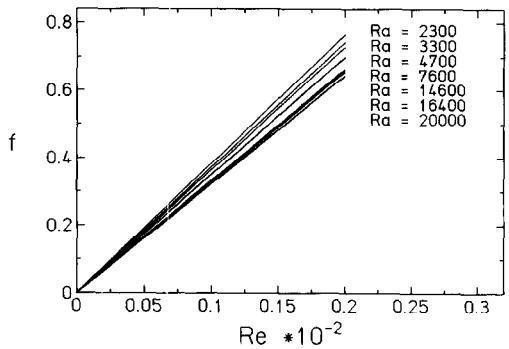

Fig. 15. Frequency as function of *Ra* and *Re*.

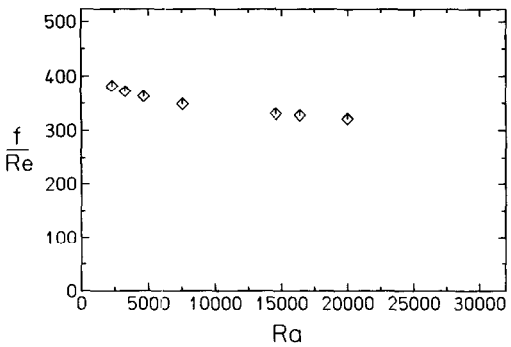

Fig. 16. Reduced frequency as function of *Ra*.

longitudinal rolls, Fig. 18. This convective state becomes stationary. The convective amplitude w_{max} is about 2–6% smaller than in the case of transverse rolls, but is still a function of the Rayleigh number, discussed under (b).

FINAL REMARKS

The formulation of inlet and outlet boundary conditions for the three-dimensional mixed convection is of great importance for the dynamical behavior of those flows. The simulation of porous sidewalls, described by a constant velocity profile, leads to phase fixing of the roll structure. Compared to long channel flows, simulated by periodic boundary conditions, the oscillation frequency is smaller, proving that porous sidewalls hinder the movement of the rolls.

The flow structure changes at high Reynolds and small Rayleigh numbers. In the short box the change from transverse to longitudinal rolls takes place continuously, where transverse and longitudinal rolls are present at the same time in different parts of the box.

In an infinitely long channel, transverse and longitudinal rolls cannot coexist like they do in a short box. The roll structure is everywhere the same along the channel length. The change from transverse to longitudinal rolls in the infinitely long channel takes place in the parameter range of $0.05 < Re < 0.1$.

Table 2. Quotient of travelling velocity and average velocity of the throughflow as function of the Rayleigh number

Source	Pr	H_y	$\frac{u_r}{\bar{u}}$
Ouazzani *et al.* [6]	0.71	∞	$\frac{u_r}{\bar{u}} = 1.70 - 1.90 \times 10^{-5} \cdot Ra$
Ouazzani *et al.* [7]	7	3.63	$\frac{u_r}{\bar{u}} = 1.62 - 8.67 \times 10^{-5} \cdot Ra$
Numerical results	530	4.1	$\frac{u_r}{\bar{u}} = 1.53 - 3.18 \times 10^{-5} \cdot Ra$

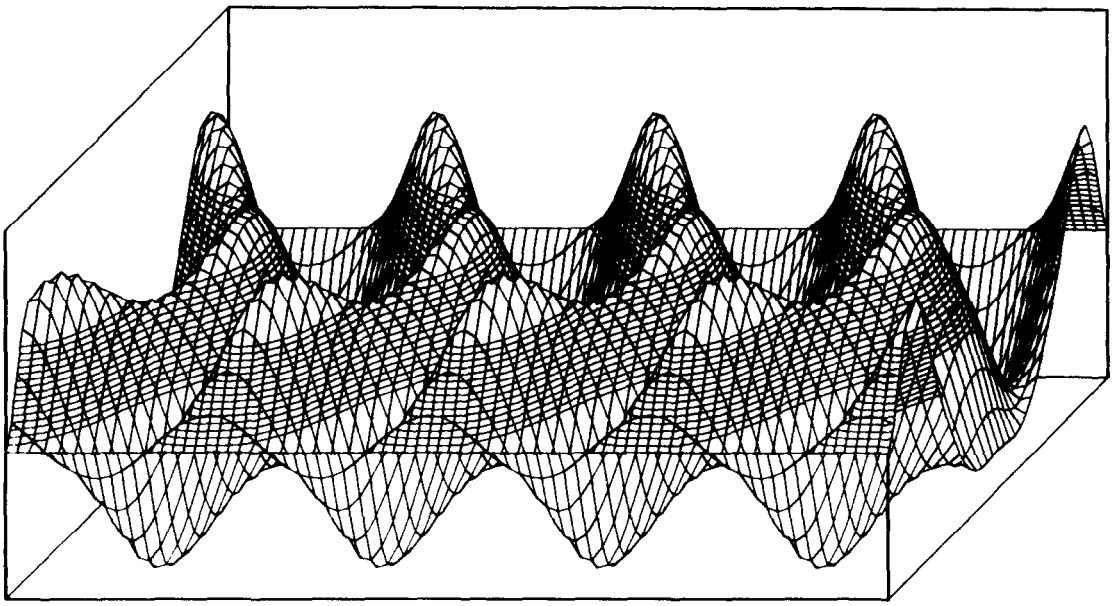

Fig. 17. Change of orientation in the long channel, $Ra = 7600$, $Re = 0.05$, $Pr = 530$.

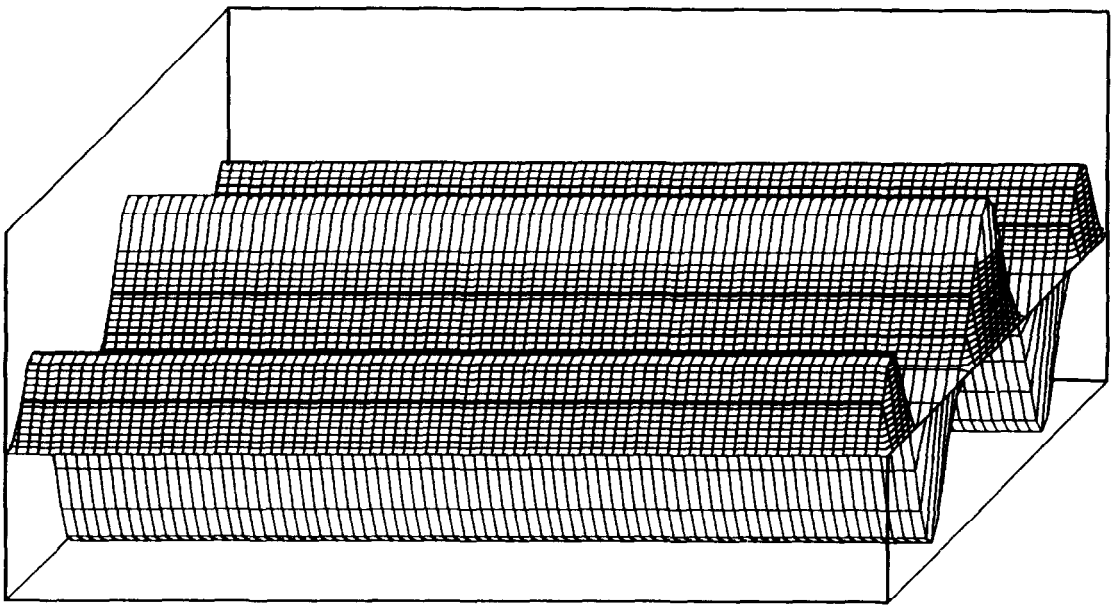

Fig. 18. Longitudinal rolls in the long channel, $Ra = 7600$, $Re = 0.1$, $Pr = 530$.

The investigations show that a three-dimensional analysis of the mixed convection is necessary if any change of the roll orientation is to be simulated. It has also been shown, that experimental and numerical results are in good agreement, in particular the flow structure and the dynamical behavior of free convection with a superimposed mass flux in a short box.

REFERENCES

1. H. K. Moffat and K. F. Jensen, Three-dimensional flow effects in silicon CVD in horizontal reactors, *J. Electrochem. Soc.* **135**(2), 459–471 (1988).
2. E. Schröder, Numerische und experimentelle Untersuchung der dreidimensionalen gemischten Konvektion in quaderförmigen Behältern und im Rechteckkanal, Dissertation, Universität Karlsruhe (TH) (1993).
3. K. Stork and U. Müller, Convection in boxes: experiments, *J. Fluid Mech.* **54**(4), 599–611 (1972).
4. J. K. Platten and J. C. Legros, *Convection in Liquids*. Springer, Berlin (1984).
5. J.-M. Luijkx, J. K. Platten and J. Cl. Legros, On the existence of thermoconvective rolls, transverse to a superimposed mean Poiseuille flow, *Int. J. Heat Mass Transfer* **24**(7), 1287–1291 (1981).
6. M. T. Ouazzani, J. P. Caltagirone, G. Meyer and A. Mojtabi, Etude numérique et expérimentale de la convection mixte entre deux plans horizontaux à températures différéntes, *Int. J. Heat Mass Transfer* **32**(2), 261–269 (1989).

7. M. T. Ouazzani, J. K. Platten and A. Mojtabi, Etude expérimentale de la convection mixte entre deux plans horizontaux à températures différéntes—II, *Int. J. Heat Mass Transfer* **33**(7), 1417–1427 (1990).
8. H. W. Müller, Thermische Konvektion in horizontaler Scherströmung, Dissertation, Universität Saarbrücken (1990).
9. H. Oertel, Jr. and K. Bühler, A special differential interferometer used for heat convection investigations, *Int. J. Heat Mass Transfer* **21**, 1111–1115 (1978).
10. A. A. Amsden and F. H. Harlow, The SMAC method : a numerical technique for calculating incompressible fluid flows, LA-4370, Los Alamos Scientific Lab., NM (1970).
11. K. R. Kirchartz, Dreidimensionale Konvektion in quaderförmigen Behältern, Habilitationsschrift, Universität Karlsruhe (TH) (1988).